13R.2 EVALUATION OF THE RANGE CORRECTION ALGORITHM AND CONVECTIVE STRATIFORM SEPARATION ALGORITHM FOR IMPROVING HYDROLOGICAL MODELING

Feng Ding[1]*, David Kitzmiller[2], David Riley[2], Kiran Shrestha[1], Fekadu Moreda[3], Dong-Jun Seo[4]

[1]RS Information Systems, Inc./Hydrology Laboratory
Office of Hydrologic Development
National Weather Service, NOAA, Silver Spring, Maryland

[2]Hydrology Laboratory, Office of Hydrologic Development
National Weather Service, NOAA, Silver Spring, Maryland

[3]MHW, Inc./Hydrology Laboratory, Office of Hydrologic Development
National Weather Service, NOAA, Silver Spring, Maryland

[4]UCAR/Hydrology Laboratory, Office of Hydrologic Development
National Weather Service, NOAA, Silver Spring, Maryland

1. INTRODUCTION

The Range Correction Algorithm (RCA) and its companion, the Convective Stratiform Separation Algorithm (CSSA), have been developed by the Office of Hydrologic Development (OHD), NOAA's National Weather Service (NWS) (Seo et al. 2000, 2002, Ding et al. 2003). The algorithms mitigate range-dependent biases in radar precipitation estimates due to nonuniform vertical profiles of reflectivity (VPR), i.e., reduce overestimates from bright band effect and underestimates from overshooting at far ranges. The internal evaluation and field evaluation of RCA/CSSA were conducted by the OHD during the period of February – May 2003 using real-time data from single radar site KLWX (Sterling, VA), and during the period of March – June 2004 using real-time data from multiple radar sites: KRTX (Portland OR), KEAX (Pleasant Hill, MO), KMPX (Minneapolis, MN), KTLX (Twin Lakes, OK), KPBZ (Pittsburgh, PA), and KRLX (Charleston, WV). The results from the evaluation have shown that the application of RCA/CSSA significantly improved rainfall estimates, in terms of agreement with rain gauge observations (Ding et al. 2004, 2005). The RCA will be a desirable estimation component even after the deployment of dual-polarization upgrades to the WSR-88D network. While dual-polarization algorithms can differentiate between snowflakes and raindrops, information on the reflectivity profile is still crucial to estimation of surface rainfall when the lowest radar beam detects only snow above the melting level.

In this study, the primary evaluation of RCA and CSSA as a means of improving hydrological forecasts was conducted by applying the NWS Hydrology Laboratory Research Modeling System (HL-RMS) to five river basins within the umbrella of the WSR-88D unit in State College, Pennsylvania (KCCX). Multisensor and radar precipitation estimates with and without range correction were input to HL-RMS in order to simulate streamflow following a rain event in January 2003. The simulation results, such as mean areal precipitation (MAP), runoff estimates, and flow hydrographs, were analyzed to show the effects of RCA and CSSA. Our first goal was to demonstrate that application of the RCA improves precipitation estimates from a single radar so that they more closely match estimates from a multiple radar and rain gauge analysis over the same area. A second goal was to show that these improvements were reflected in hydrologic simulations of streamflow.

The organization of this paper is as follows. In section 2, HL-RMS and the study area were described. In section 3, the details of precipitation data set were given. In section 4, the simulation results were presented. Section 5 provided conclusions.

2. HL-RMS AND THE STUDY AREA

HL-RMS is a flexible hydrological modeling system developed by HL of OHD, NOAA's NWS (Koren et al. 2004). It consists of a well-tested conceptual water balance model applied on a regular spatial grid linked to physically-based kinematic hillslope and channel routing models. In the framework of HL-RMS, the SNOW-17 model was used to estimate snowmelt. The Continuous Antecedent Precipitation Index (CONT-API) model was used to convert the rain+melt into runoff in each grid. Hillslope and channel routing were accomplished using a kinematic wave model.

The rainfall-runoff model generates fast (surface) and slow (subsurface/ground) runoff components. Within each grid, fast runoff was routed over conceptual hillslopes to a channel, and then this channel inflow was combined with the slow runoff component. Outflows from upstream pixel are routed through a pixel conceptual channel. The cell-to-cell connectivity sequence was pre-determined in order to move water from upstream to downstream grids and to the basin

* *Corresponding author address:* Feng Ding, W/OHD-12, 1325 East West Highway, Silver Spring, MD 20910; email: feng.ding@noaa.gov

outlet. The *a priori* parameters derived by Moreda et al. (2005), were used for the CONT-API and routing models. For the SNOW-17 model, lumped operational parameters were used.

The study area consists of 5 basins within the umbrella of the KCCX radar. Figure 1 shows the locations of 5 basins with radar site, 100km, 200km and 300km range rings indicated. Table 1 lists the basins' identifiers, areas, distances from the radar site, and rivers' names. The basins are centered at several different ranges from KCCX.

3. PRECIPITATION DATA SETS

Precipitation data input to HL-RMS were generated from KCCX radar data and rain gauge observations. Five types of precipitation data were input to HL-RMS for the simulations. All of them, described below, are hourly precipitation, mapped to the Hydrologic Rainfall Analysis Project (HRAP) grid system, which has the resolution of about 4km by 4km.

We denote the reference precipitation analysis as OPERATION since it is a radar-gauge multisensor field prepared operationally at the Mid-Atlantic River Forecast Center (MARFC). It is obtained by optimally merging rain gauge and mean field bias (MFB) corrected radar rainfall after manual quality control (Seo 1998). The OPERATION estimates are based on information from multiple radars and a dense rain gauge network, and thus are superior to the radar-only KCCX estimates.

The first radar estimate is radar-only precipitation without RCA/CSSA correction, from hourly Digital Precipitation Array (DPA) referred to as DPA hereafter. The second is radar precipitation with RCA/CSSA correction, hereafter referred as DPR. To obtain DPR, the RCA/CSSA product Adjustment Factors Array (AFA), was first generated by running RCA/CSSA added Open Radar Product Generation (ORPG) system using radar level II base data ordered from National Climate Data Center (NCDC) archives. The AFA consists of an array of multiplicative factors, based on the mean vertical profile of reflectivity, that adjusts radar rainfall rates to compensate for bright band and range degradation effects. The DPR was computed by applying AFA to DPA.

The third and fourth radar-based estimates are same as the first and second ones except MFB correction is applied. MFB correction is to remove the systematic bias due to radar calibration problem, Z-R parameters, etc. (Seo et al. 1999). The bias adjustment factors are based on an hour-by-hour comparison of the DPA and DPR products to the operational multisensor product described below. For any hour, the bias factor is the sum of all nonzero multisensor estimates divided by the sum of all nonzero radar estimates. All radar estimates are then multiplied by this single bias factor, insuring that the umbrella-mean radar rainfall is equal to the umbrella-mean multisensor value. The resulting estimates are referred as DPA-MFB and DPR-MFB. Because the bias adjustment is done hourly, and because precipitation intensity and coverage varies during the storm event, the MFB correction does not insure that the radar estimates at any one place, nor the storm-total estimates, are unbiased.

The study is focused on the heavy precipitation event of January 1 – 2, 2003, which resulted in more than 80mm rainfall in 22 hours (09Z of Jan. 1 to 06Z of Jan. 2) at some places. Figure 2 shows DPA-MFB, DPR-MFB, and OPERATION precipitation fields, respectively. It can be seen that significant range dependent bias existed in DPA-MFB field. The overestimated rainfall band in the mid-range of radar umbrella was obviously from the typical bright band effect. After RCA/CSSA correction, the DPR-MFB field showed much evenly-distributed rainfall over the radar umbrella with mid-range overestimates well-reduced and some mitigation of far-range underestimation due to radar beam overshooting. A comparison of DPA-MFB and DPR-MFB to OPERATION indicated that rank correlation was increased from 0.51 for DPA-MFB to 0.63 for DPR-MFB, and Root Mean Square Error (RMSE) was decreased from 20mm for DPA-MFB to 12mm for DPR-MFB. These results are for the KCCX umbrella as a whole.

4. SIMULATION RESULTS

Note that we did not compare any of the HL-RMS simulation results to operational forecasts made with NWSRFS or to streamflow observations. Tests showed that further calibration would be necessary in order to obtain accurate simulations in an absolute sense. Our aim here is to isolate calibration effect from RCA/CSSA correction effect.

Therefore we carried out the experiment by comparing the radar-based simulations to the reference simulations based on the OPERATION precipitation analysis, which was, as noted above, almost certainly closer to ground truth than any of the radar-based estimates. Our aim was to show that with range and MFB correction, radar estimates and hydrologic simulations from KCCX precipitation alone more closely approximated the results based on the radar-mosaic and gauge precipitation OPERATION field. Of course, this study could not demonstrate that precipitation estimates from KCCX alone will serve as a useful surrogate for the existing radar and rain gauge network in central Pennsylvania. We can demonstrate that range and MFB correction will be useful in areas with only a sparse gauge network and coverage from only one WSR-88D.

While the storm event of January 1 to 2, 2003 is the focus of this study, HL-RMS was run with 5 months of data (from September 1, 2002 to January 31, 2003) for enough spin up time. Five simulations were conducted with 5 types of precipitation input in each basin. One

used 5 months OPERATION precipitation. The other four used 22 hours of DPA, DPR, DPA-MFB, and DPR-MFB plugged in the OPERATION precipitation, respectively. Again, there are referred as OPERATION run, DPA run, DPR run, DPA-MFB run, and DPR-MFB run.

4.1 Basin mean-areal precipitation (MAP)

The comparison of MAP for the 5 estimates for each basin is shown in Figure 3. It can be seen that in all 5 basins MAPs from DPA and DPR are less than MAP from OPERATION. It means that raw radar precipitation was a serious underestimate, a common situation in the cold season. The MFB correction applied here approximately doubled the raw estimates.

MAPs from four basins (SPKP1, WLBP1, SXTP1, and LWVP1), showed similar patterns. With and without MFB correction, due to the overestimation from bright band effect, MAP from DPA/DPA-MFB was greater than that from DPR/DPR-MFB, particularly in basin SXTP1, located at about 120 km from KCCX radar site. In SPKP1 and WLBP1 basin, even though MAPs from DPA seemed closer to those from OPERATION, it was because the large MFB values (about 2 or double the raw precipitation) counteracted the significant overestimation from bright band effect. MAPs from DPR-MFB were better than MAPs from DPA-MFB. In SXTP1 and LWVP1 basin, MAPs from DPR-MFB were definitely the closest to MAPs from OPERATION. In the SXTP1 basin, which is the largest basin, MAP from DPR-MFB (1.861mm) was about the same as MAP from OPERATION (1.867mm).

CRNN6 was a basin relatively far away (170km) from KCCX radar site. The DPA suffered from the beam overshooting herein underestimated precipitation. RCA/CSSA correction mitigated such underestimation somewhat, nevertheless not as significantly as the correction of overestimation from the bright band effect. In CRNN6 basin, even though MAP from DPR-MFB was much less than MAP from OPERATION, it was obviously better than others. Note that the OPERATION estimates in this area were from a closer radar and gauge reports. Therefore, in CRNN6, MAP from OPERATION was much greater than others.

In terms of percentage error relative to the OPERATION analysis (Figure 4), it can be seen that the DPR-MFB had a consistently smaller error than that of the DPA-MFB. For the SXTP1 and LWVP1 basins, the DPR-MFB percentage error was < 10%. For the reasons noted above, the percentage error for DPA was sometimes smallest of all. However, after the MFB adjustment was applied to bring the umbrella-wide DPA into better balance with rain gauge estimates, the lack of range correction caused DPA-MFB to be 30-60% too high in all basins except CRNN6.

In summary, the results of comparing MAPs in all basins were consistent with the precipitation fields shown in Figure 2.

4.2 Simulated Hydrographs

The hydrographs for the five test basins for the period 1 – 16 January, and all five forms of precipitation input, are shown in Figures 5 – 9. In all five basins, it was found that peak flow values of both DPA and DPR run were less than that of OPERATION run, and DPA run was closer to OPERATION run in most basins. Thus range correction alone did not improve the radar estimates in this event. This is because most of the basins were under or near the zone of bright-band enhancement, which partly counteracted the overall underestimation in the DPA product. While range correction mitigated this bright-band effect, improving the representation of the spatial pattern of precipitation, it also made the underestimation more serious over these basins. This effect is substantially compensated with MFB correction, and as will be shown, the flow simulations with both range and MFB correction were closer to the reference simulations.

Like MAPs, hydrographs of SPKP1 (Figure 5) and WLBP1 (Figure 6) basin were quite similar. The peak flow time of all 5 runs were almost same (less than 4 hours difference). Although the peak flow values of both DPA-MFB and DPR-MFB runs were significantly greater than that of OPERATION run, the peak flow value of DPR-MFB run was much closer to that of OPERATION run. If the peak flow of OPERATION run is treated as the “truth”, then in SPKP1 basin, the absolute error (AE) of peak flow was reduced from 38.55m^3/s for the DPA-MFB run to 20.13m^3/s for the DPR-MFB run, and the relative error (RE) of peak flow was reduced from 69.4% to 36.3%. In WLBP1 basin, the improvement was even distinct. The AE of peak flow was reduced from 103.44m^3/s for the DPA-MFB run to 34.94m^3/s for the DPR-MFB run, and the RE was reduced from 127.4% to 43.0%.

In SXTP1 basin (Figure 7), in addition to the very good MAP from the RCA/CSSA plus MFB correction, the hydrograph of DPR-MFB run was extremely good as well. Two flow curves of DPR-MFB run and OPERATION run were almost coincided with the exception of peak flow time of DPR-MFB run was 4 hours later than that of OPERATION run, and peak flow value of 0.33m^3/s less. On the other hand, the peak flow of DPA-MFB run was markedly overestimated, with the AE and RE 139.45m^3/s and 69.7%. This case is nearly a “perfect case” to prove the improvement from the RCA/CSSA and MFB correction.

Even not as good as the SXTP1 basin, the hydrograph in LWVP1 basin (Figure 8) also showed improvement from RCA/CSSA and MFB correction. The flow cure of DPR-MFB run was the closest one to the OPERATION run than other runs. Compared to DPA-MFB run, the AE and RE of peak flow of DPR-MFB run

were reduced from 55.50m^3/s to 30.17m^3/s, and from 39.8% to 21.6%. The large area of SXTP1 basin may cause the simulated flow better that LWVP1 basin.

Basin CCRN6 is the only basin in which RCA/CSSA made an upward correction due to radar beam overshooting at far ranges. Figure 9 shows the hydrograph of this basin. It could be seen that compared to OPERATION run, the peak flow time of other runs was obviously delayed, up to 9 hours. It was also found that peak flow of DPA-MFB run was greater than that of DPR-MFB run, hence closer to OPERATION run, which was contrary to the MAP result in Figure 2. From the MAP, it would be expected that peak flow of DPA-MFB run was less than that of DPR-MFB run. The reason to cause this apparently contradictory is that CRNN6 is a downstream basin, rather than a headwater like the others. LWVP1 is one of the upstream basins which mainly contributed to the flow in CRNN6 basin. Since in LWVP1 basin the flow of DPA-MFB run was much greater than the flow of DPR-MFB run, as mentioned above, the flow of DPA-MFB run was also greater than that of DPR-MFB run in CRNN6 basin. To isolate the net flow in CRNN6 basin, a simple approximation was done by subtracting flow in the LWVP1 basin from that in the CRNN6 basin, not considering routing of channel flow. In terms of peak flow, this suggested that the net peak flow of DPA-MFB run was 59.86m^3/s, DPR-MFB run 83.45m^3/s, and OPERATION run 147.65m^3/s. Thus, it turned out that net peak flow DPR-MFB run was closer to OPERATION run, which was again consistent with MAP result. This proved that the mitigation from the RCA/CSSA for the overshooting at far ranges could also improve the hydrological modeling, like the RCA/CSSA correction to bright band effect.

4.3 Flow error statistics

Though it is apparent that for three of the basins none of the radar precipitation estimates provided a very close approximation to either the reference MAP (Figure 3) or the reference streamflow (Figures 5,6, and 9), it should be noted that the application of range and MFB correction did result in improvement in 4 out of 5 cases and in good simulations for the SXTP1 and LWVP1 basins (Figures 7 and 8). The improvement is more apparent in terms of percentage error in total runoff (Figure 10a), which was approximated as the percentage error in total discharge between 1 and 6 January. As with MAP, the DPR-MFB had a percentage error < 10% for SXTP1 and LWVP1, and was noticeably poorer than DPA only in CRNN6. Similar results were evident for percentage error in peak discharge (Figure 10b). Even for CRNN6, as noted above, after correction for inflow from basin LWVP1 the percentage error in peak flow was smaller for DPR-MFB than for DPA-MFB (44% vs. 59%).

5. CONCLUSIONS

The primary evaluation of RCA/CSSA for improving hydrological modeling was conducted by running HL-RMS model using different precipitation fields in the five basins under the KCCX radar umbrella. The study was focused on the storm event of January 1 – 2, 2003. Analysis of precipitation fields, MAPs, and hydrographs indicate the following:

1. The RCA/CSSA noticeably corrected the precipitation overestimation from bright-band effect and mitigated underestimation from beam overshooting. The MFB correction can remove the systematic biases due to radar calibration problem, Z-R parameters, etc., but not the range dependent bias. RCA/CSSA plus MFB correction generally yielded the better precipitation estimate closest to the OPERATION precipitation estimate. It is expected that OPERATION precipitation estimates will also be improved if obtained from radar precipitation with RCA/CSSC correction.
2. The improvement of RCA/CSSA and MFB correction was clearly shown in the MAP results. MAP results were consistent with the precipitation field. Better precipitation estimates yields better MAP for hydrological modeling.
3. Improvements in MAP were reflected in improvements in hydrologic simulations, in terms of total runoff and storm peak discharge. The run with RCA/CSSA plus MFB correction was much better than that without RCA/CSSA correction. The improvement was considerable in terms of AE and RE of peak flow. In two of the five test basins (SXTP1 and LWVP1), the simulated flow of DPR-MFB run was very close to that of the OPERATION precipitation.

In the future, the evaluation will be extended by using a calibrated hydrological model and utilizing multiple radar-estimated precipitation sources for the entire September 2002 – January 2003 period. The longer period of record will enable us to draw firmer conclusions about the value of range correction in radar precipitation estimation.

ACKNOWLEDGMENTS

This work was supported by the National Weather Service Radar Operations Center through its Memorandum of Understanding with the Office of Hydrologic Development.

References

Ding, F., et al. 2003: Annual report of Office of Hydrologic Development to the Radar Operations Center [available from Office of Hydrologic Development, or through web site at www.nws.noaa.gov/oh/hrl/papers/papers.htm#wsr88d].

Ding, F., D-J Seo, and D. Kitzmiller, 2004, Validation of Range Correction Algorithm using real-time radar data from Sterling, VA. *18th Conference on Hydrology, American Meteorological Society*, January 9-13, 2004, Seattle, WA, **J1.5**

Ding, F., D. Kitzmiller, D-J Seo, D. Riley, C. Dietz, C. Pham, and D. Miller, 2005, A multi-site evaluation of the Range Correction and Convective-Stratiform Separation Algorithms for improving WSR-88D rainfall estimates. *19th Conference on Hydrology, American Meteorological Society*, January 9-13, 2005, San Diego, CA, **P2.11**

Koren, V., Reed, S., Smith, M., Zhang, Z., Seo, D. J., 2004: Hydrology Laboratory Research Modeling System (HL-RMS) of the National Weather Service. *J. Hydrology*, **291**, 297-318.

Moreda, F., Koren, V., Zhang, Z., Reed, S., Smith, M., 2005: Parameterization of distributed hydrological models: learning from the experiences of lumped modeling. *(In press, J. Hydrology).*

Seo, D. J., 1998: Real-time estimation of rainfall fields using radar rainfall and rain gauge. *J. Hydrology*, **208**, 37-52

Seo, D.-J., J. Breidenbach, and E.R. Johnson, 1999: Real-time estimation of mean field bias in radar rainfall data. *J. Hydrology*, **223**, 131-147.

Seo, D.-J., J. Breidenbach, R. Fulton, and D. Miller, 2000: Real-time adjustment of range-dependent biases in WSR-88D rainfall estimates due to nonuniform vertical profiles of reflectivity. *J. Hydrometeorology*, **1**, 222-240.

Seo, D.-J., et al. 2002: Annual report of Office of Hydrologic Development to the Radar Operations Center [available from Office of Hydrologic Development, or through web site at www.nws.noaa.gov/oh/hrl/papers/papers.htm#wsr88d].

Table 1. Details of five study basins

No	Basin ID	River Name	Area (km^2)	Distance from KCCX (km)
1	SPKP1	Lit jun r-spruce ck	854	50
2	WLBP1	Jun r.-williamsburg	754	75
3	SXTP1	Frnk.br.jun-saxton	1,954	120
4	LWVP1	Cowan-lawrenceville	784	140
5	CRNN6	Chemung r at corning (tot area 5,273 km2)	1,077	170

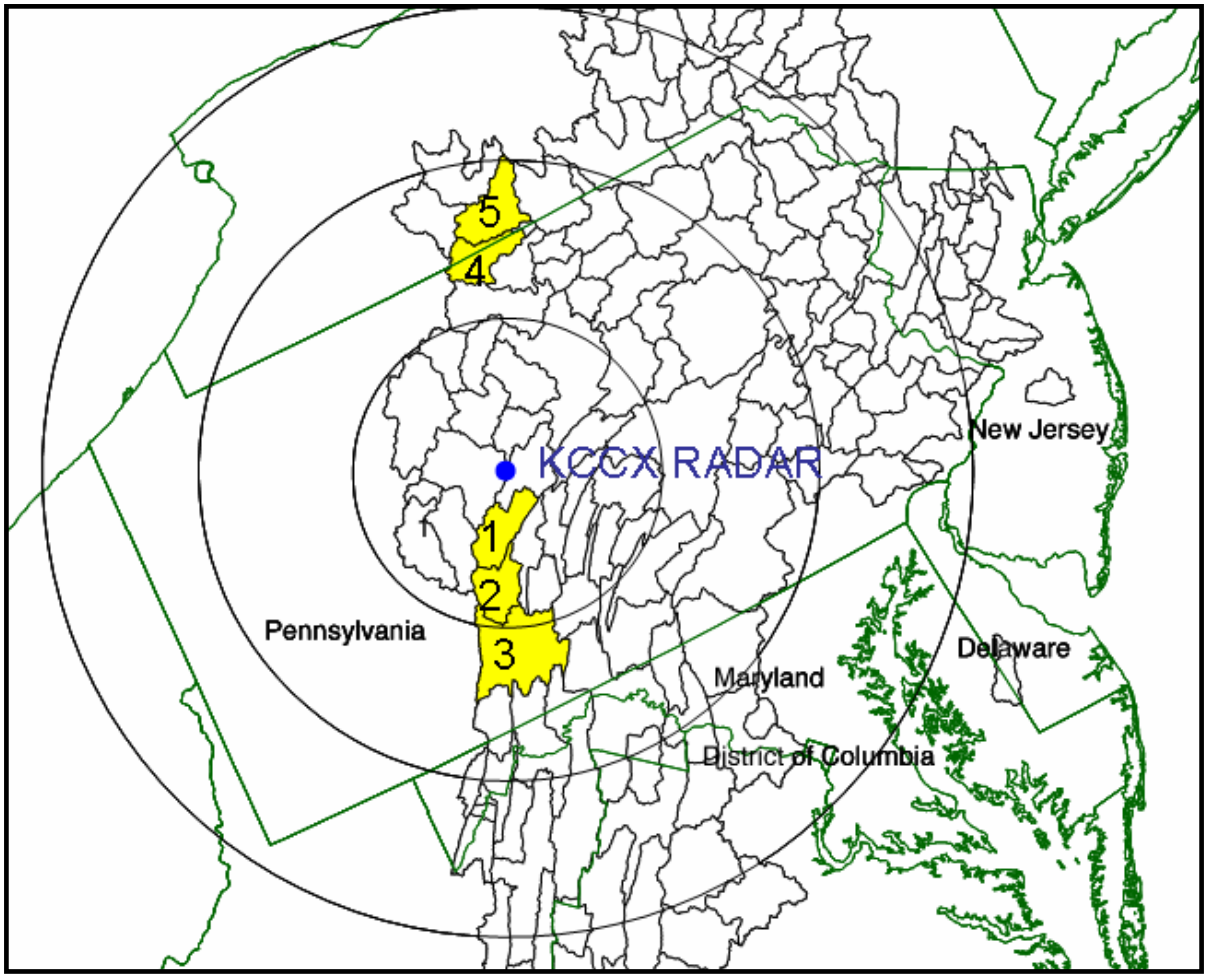

Figure 1. The map of study area. KCCX radar and 100km, 200km , and 300km rings are shown.

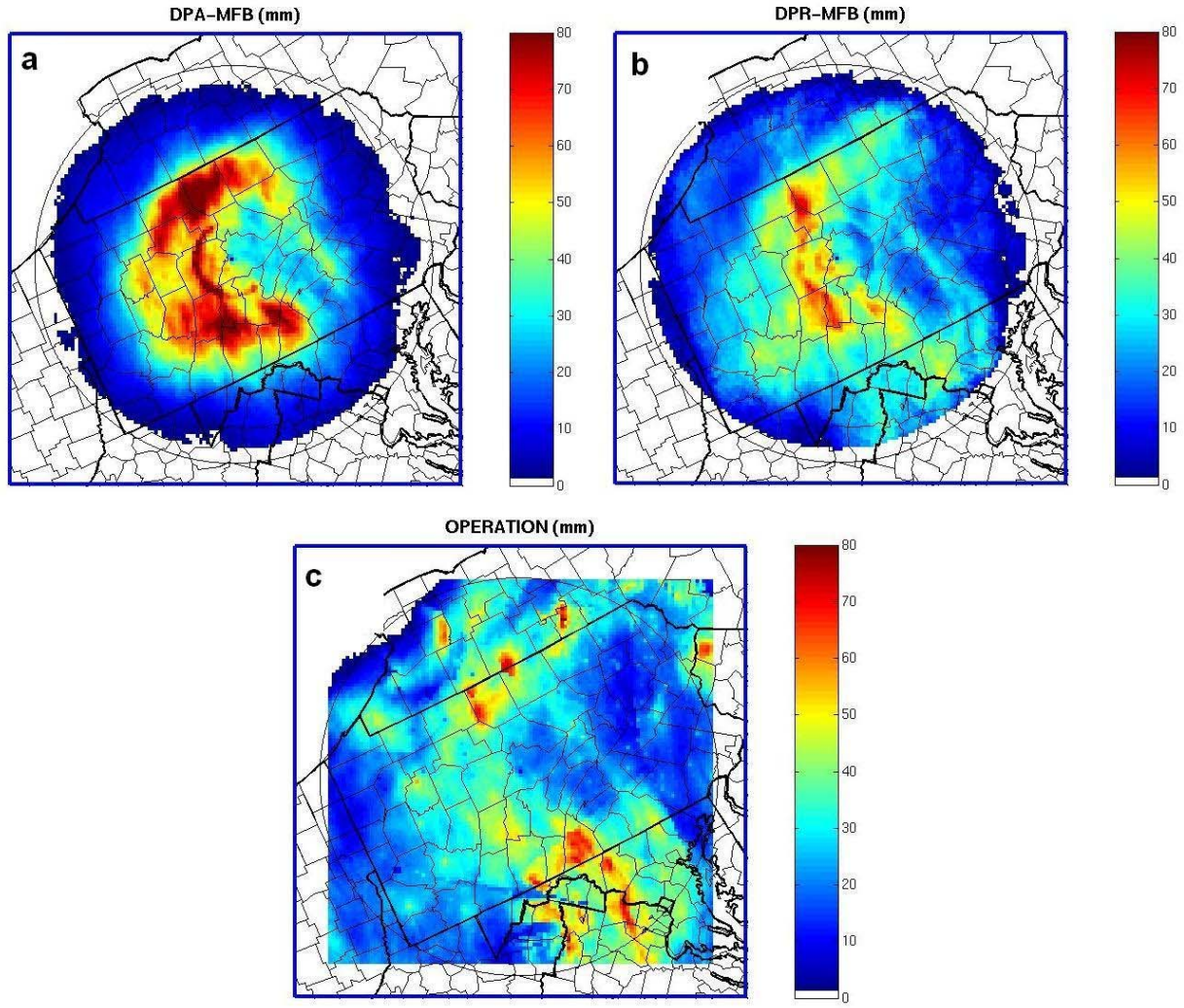

Figure 2. Storm-total precipitation estimates for the 22-hour period ending 0600 UTC 2 January 2003. Estimates are from (a) KCCX DPA with mean field bias adjustment, (b) KCCX DPR with mean field bias adjustment, and (c) operational radar/gauge mosaic prepared at Mid-Atlantic River Forecast Center.

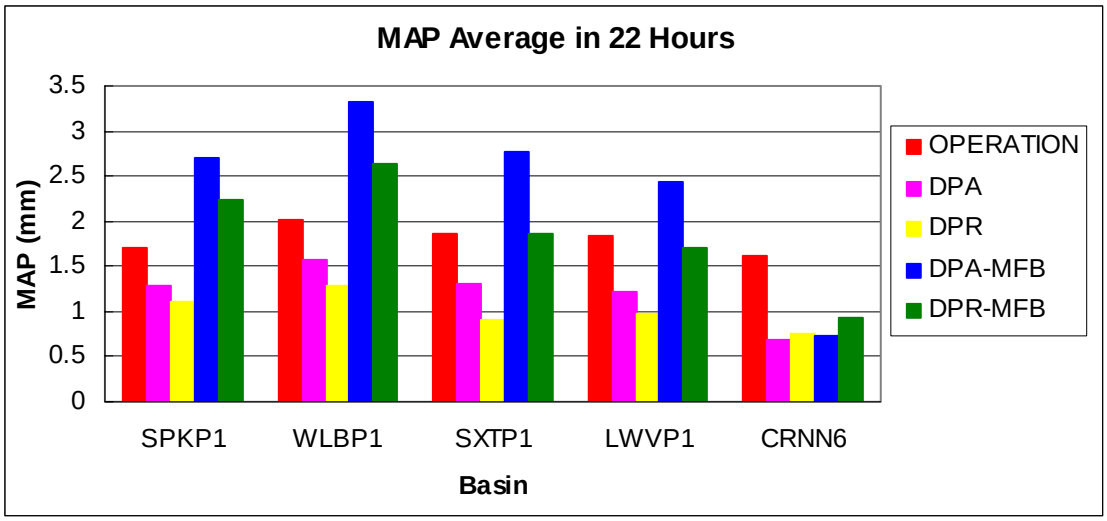

Figure 3. Storm-total MAP estimates for each basin for the 22-h period ending 0600 UTC, 2 January 2003.

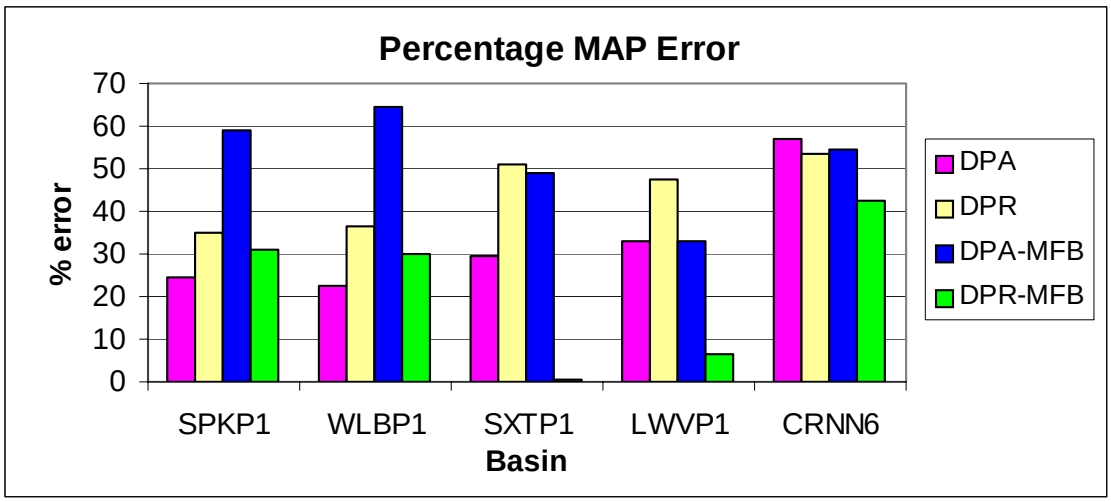

Figure 4. Percentage error in MAP estimates, relative to the Operational estimate field. The DPR-MFB error for the SXTP1 basin was < 1%.

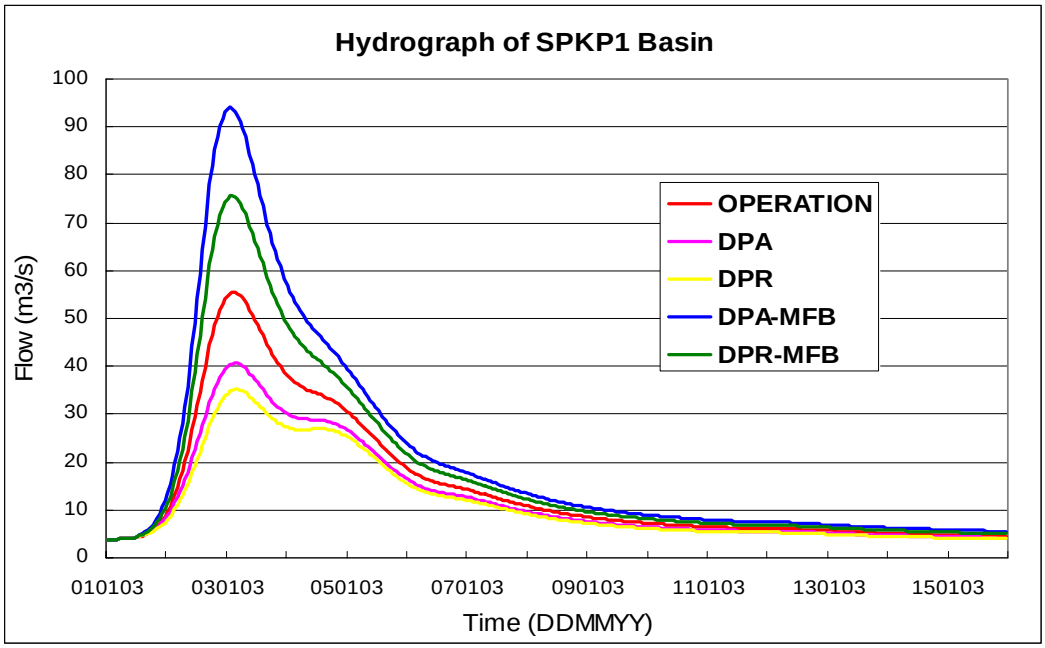

Figure 5. Comparison of hydrograph (01/01/2003 to 16/01/2003) for different precipitation input in SPKP1 basin.

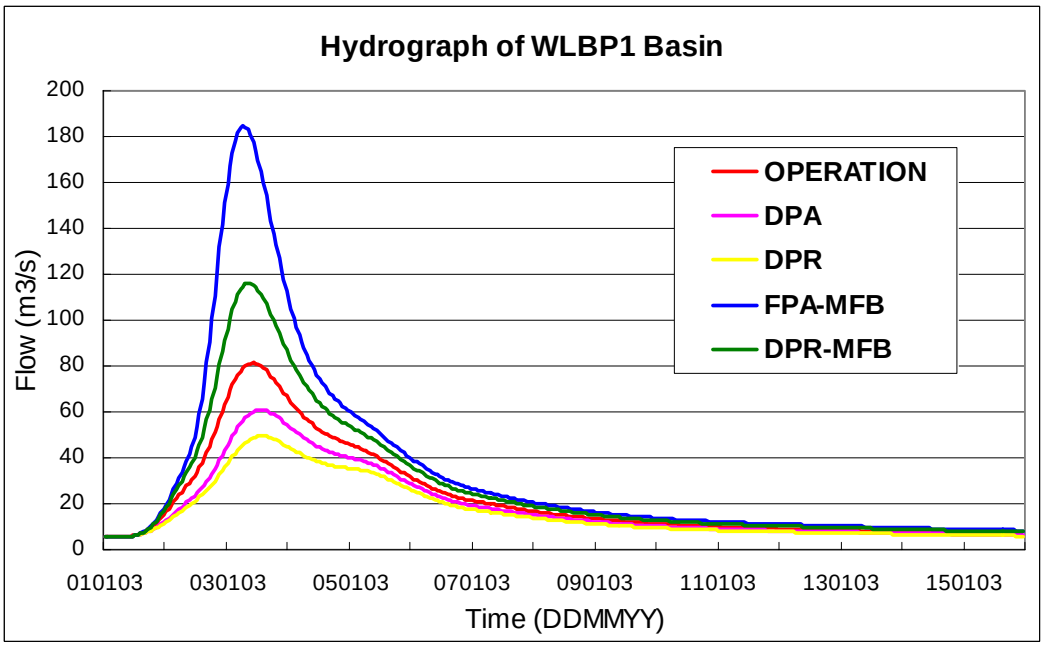

Figure 6. As in Figure 5 except for WLBP1 basin.

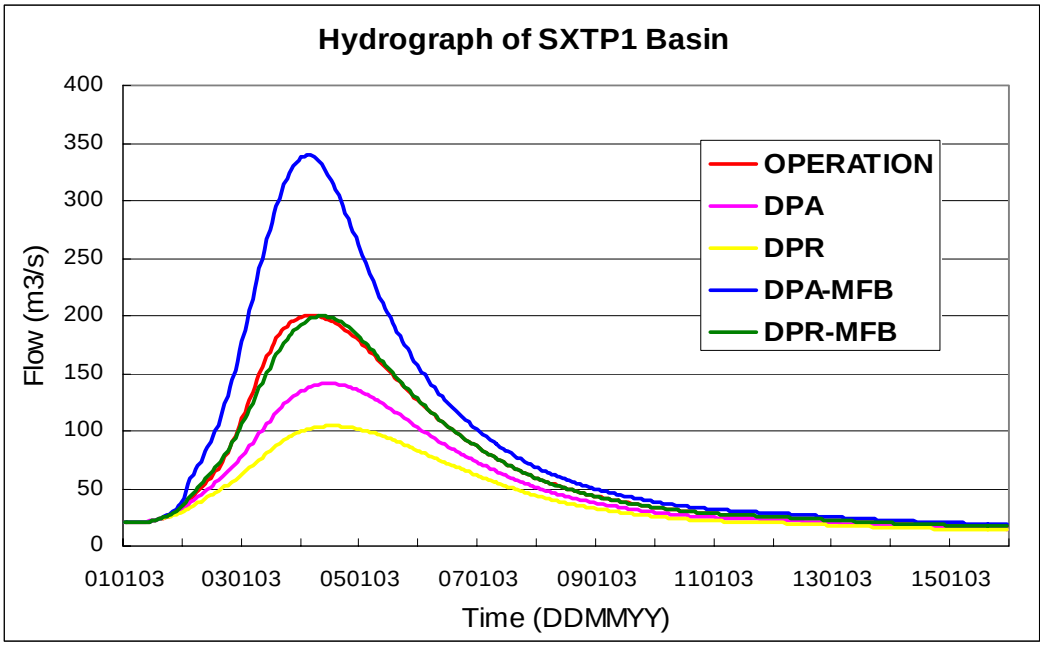

Figure 7. As in Figure 5 except for SXTP1 basin.

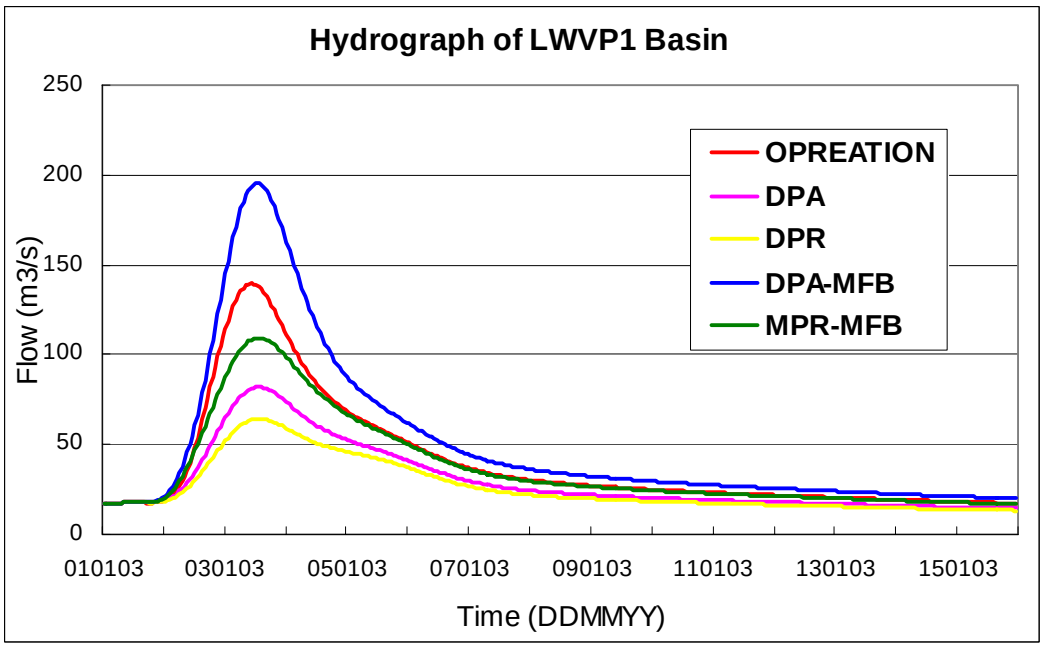

Figure 8. As in Figure 5 except for LWVP1 basin.

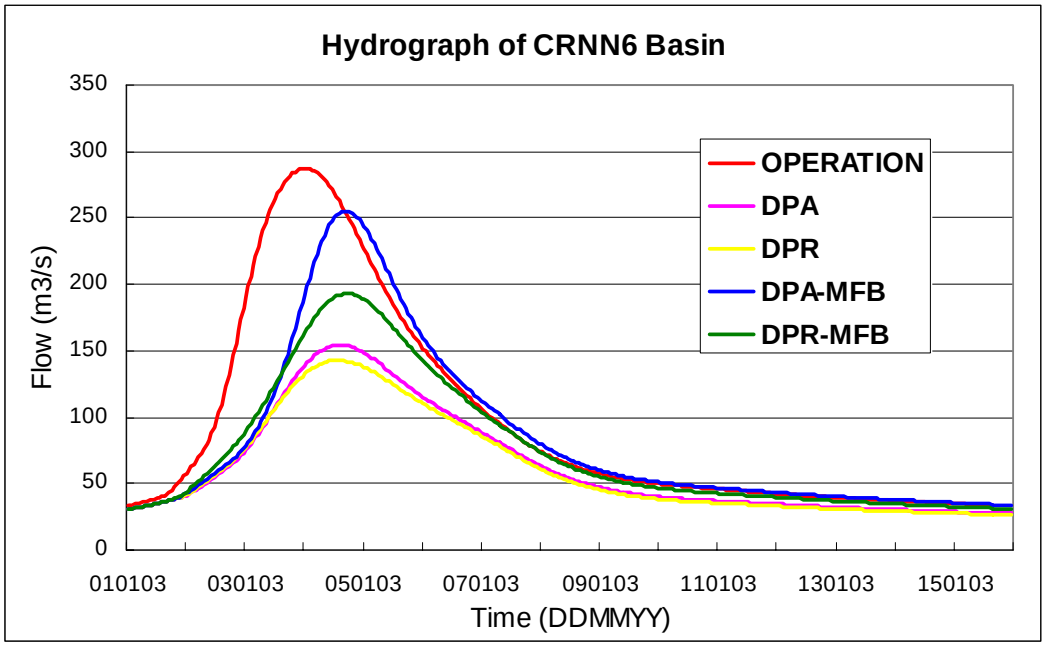

Figure 9. As in Figure 5 except for CRNN6 basin.

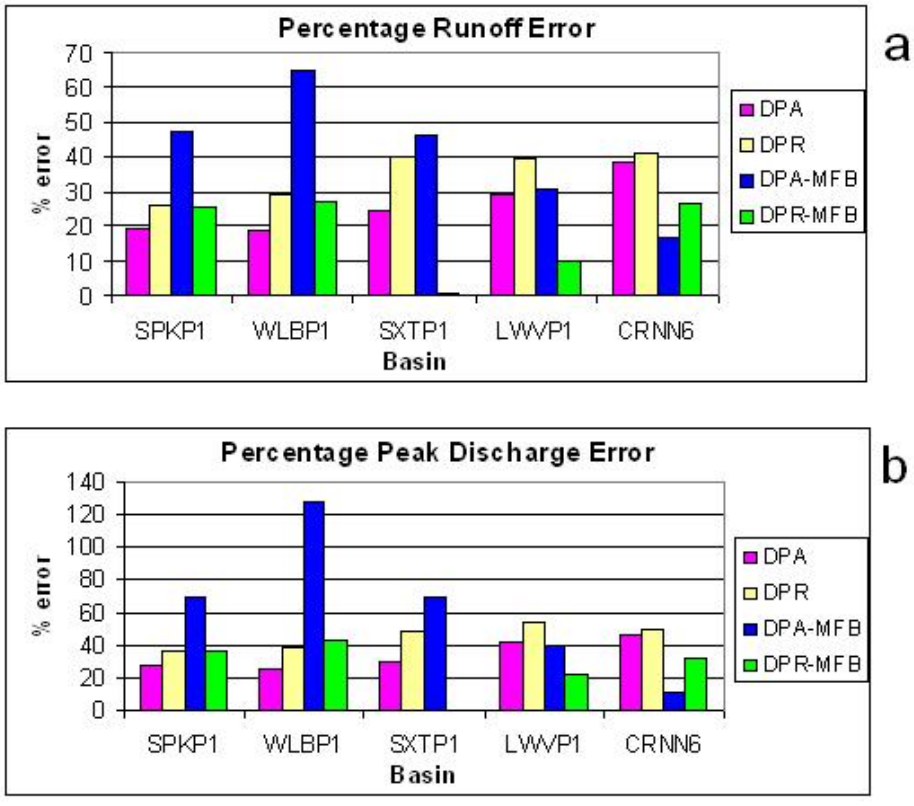

Figure 10. Percentage errors in streamflow simulations for different precipitation estimates, relative to simulation based on the Operational precipitation analyses. Percentage errors are for (a) total surface runoff and (b) peak discharge. Percentage errors for DPR-MFB for the SXTP1 basin are < 1% for both terms.